

Observed Interannual Variability and Projected Scenarios of Drought using Drought Indicators

Nitesh Gupta¹, Shivani Gond², Jitendra Patel³, Padam Jee Omar⁴, and Ravi P. Tripathi⁵ (2025)

¹*Dept. of Civil Engineering, Institute of Technology, Nirma University, India*

²*Centre for Technology Alternative for Rural Areas, Indian Institute of Technology, Bombay, India*

³*Dept. of Civil, Chemical, Environmental, and Material Engineering, Alma Mater Studiorum, Università di Bologna, Bologna, Italy*

⁴*Dept. of Civil Engineering, Babasaheb Bhimrao Ambedkar University, Lucknow, India*

⁵*Dept. of Civil Engineering, Rajkiya Engineering College, Sonbhadra, India*

DOI: <https://doi.org/10.14796/JWMM.H536>

ABSTRACT

The observation-based analysis of drought development in the Uttar Pradesh region in India showed that, despite the area being relatively large, agricultural drought exhibits high spatial variability. However, the lack of net radiation data hinders the capacity to provide reliable estimates of evapotranspiration (ET), affecting the assessment of drought occurrence since its propagation across the hydrological system becomes very sensitive to the estimation of ET. The most prominent precipitation deficits occur during the monsoon season (June to October), showing that changes in the large-scale circulation are responsible for the impact of severe drought. El Niño-Southern Oscillation (ENSO) modulates the variability of drought with a warm phase favoring drought development with the strongest influence between August and October. The climate change projections under RCP4.5 and RCP8.5 scenarios suggest the intensification of drought events in the Uttar Pradesh region in the mid-century, with the Chambal River of the Ganges River basin being the most affected area in terms of precipitation and temperature. The projected scenarios correspond to an increase of 1.7°C for mean temperature, and 3.5°C for minimum and maximum temperature in the 2050 horizon, and a decrease of 400 to 800 mm for annual precipitation was projected under both RCPs.

Gupta, N., S. Gond, J. Patel, P.J. Omar, and R.P. Tripathi. 2025. "Observed Interannual Variability and Projected Scenarios of Drought using Drought Indicators." *Journal of Water Management Modeling* 33: H536. <https://doi.org/10.14796/JWMM.H536> www.chijournal.org ISSN: 2292-6062 © Gupta et al. 2025.



This work is licensed under a Creative Commons Attribution 4.0 International License

1. INTRODUCTION

Droughts are among the most damaging natural hazards given their impact on ecosystems, agriculture, human livelihood, and economic cost to society (Gond et al. 2023; Schwalm et al. 2017; Meza et al. 2020). It encompasses various forms such as meteorological, hydrological, agricultural, and human-induced droughts. India experiences drought in both high and low rainfall regions. Around 68% of the nation's area is susceptible to drought across different degrees. Regions receiving rainfall ranging from 750 to 1125 mm, making up 35%, are deemed prone to drought, while 33% receiving less than 750 mm face chronic drought conditions (Pandey et al. 2022). Water scarcity issues even extend to the Himalayan region. Historically, India has confronted severe droughts that exerted enduring effects on water resources, agriculture, the economy, and societal well-being (Jee et al. 2019; Mishra and Singh 2010). Certain historical droughts in India led to famines resulting in the loss of millions of lives (Mishra et al. 2019). Notably, the 2015 drought impacted crop yields and water availability in the Indo-Gangetic Plain and Maharashtra region (Mishra et al. 2016). Another case in 2015–2016 brought about substantial depletion of groundwater in the Indo-Gangetic plains and southern states, affecting approximately 330 million people across 10 states (UNICEF 2016). Deficits in terrestrial water storage were particularly severe during the droughts of 2004, 2009, and 2012, reaching a peak in the Ganges basin in 2009 (Goldin 2016). Hence, effective monitoring, assessment, and quantification of droughts are vital for the successful evaluation and implementation of mitigation strategies. In their study, Jain et al. (2015) focused on evaluating vulnerability to drought through the Integrated Drought Vulnerability Index.

Drought is associated with a prolonged decrease in water availability (Van Loon et al. 2016). The absence or reduction of rainfall (meteorological drought) combined with the increase in atmospheric demands, can be sustained in time and propagate to affect other components of the hydrological system (Miralles et al. 2019; Pandey et al. 2023). During rainfall deficit conditions, the content of soil moisture is immediately affected due to evaporation, infiltration, and root subtraction losses (Jodhani et al. 2023). As soil moisture content drops below normal-average values, an agricultural drought develops, and the decrease in water supply for the vegetation is linked to crop losses (Srivastava et al. 2023; Van Loon and Laaha 2015). If these conditions persist and reach the saturated section of the soil (groundwater reservoirs), a hydrological drought develops (Singh et al. 2022). As a dry event evolves, actual evapotranspiration decreases as a function of the soil moisture content deficit (Guguloth and Pandey 2023). These relationships are regulated by ecosystem conditions such as soil moisture, and aerodynamic and radiative properties, and by conditions that are specific to the vegetation cover and include root depth, and regulation of stomatal conductance (Miralles et al. 2019). Vegetation under water stress exhibits a change in photosynthesis and its capacity to provide the transpiration required by the atmospheric demand. The magnitude of these changes varies depending on the specific characteristics of the ecosystems (Cooley et al. 2018; Jain et al. 2023). The assessment of drought evolution is limited by the complexity of the surface interactions and the role of surface-atmosphere feedback mechanisms in the system, which added to the condition of the ecosystems, plays a major role in the occurrence and evolution of rainfall extremes (Gaur et al. 2023; Miralles et al. 2019). ET considers the loss of water from the soil (evaporation) and the transpiration of the plants (Jodhani et al. 2024); it also represents a complex variety of processes that are strongly connected to local conditions (McCabe et al. 2019). Evapotranspiration (ET) exhibits a different response to the onset and development of a dry event, which can modify the atmospheric conditions and enhance the severity of the drought (Miralles et al. 2019). ET can be considered as an aridity indicator using the variability of the ratio between precipitation (P) and Potential Evapotranspiration (PET). Given the importance of ET to link the surface and atmosphere in terms of the transport of energy, water, and carbon, different methods have been

developed that include direct measurements (lysimeter, evaporimeter tank, eddy covariance systems), indirect (Thornthwaite, Hargreaves, and Penman-Monteith equations), and remote sensing (based on satellite products such as Landsat and Terra) (Omar and Kumar 2021). The indirect methods are based on surface temperature or radiation as PET estimation is driven by energy, thus omitting available water in the surface. However, the direct method considers the mass balance (Chaware et al. 2017) and does not solve the issue of the influence of the vegetation and soil moisture content. Penman-Monteith approximation (Monteith 1965) is a relatively precise method that integrates the different processes that account for ET. During the development of a dry event, low relative humidity is dominant, cloudiness is reduced, and air is warm, hence a high atmospheric demand promotes surface evaporation. Those conditions, together with the precipitation-deficit regions, result in a sustained reduction of soil water content to the point in which soil moisture reaches values below the reference threshold (critical soil moisture), resulting in the evolution of a drought (Miralles et al. 2019). In addition, the water deficit also affects vegetation, because the transpiration flux is a function of soil moisture and consequently the water availability for evaporation is decreased (Jodhani et al. 2023). Sensible and latent heat changes contribute to variations in the temperature and humidity of the boundary layer and have a direct influence on cloud formation and rainfall because of the surface-atmosphere coupling. ET plays a role in the modulation of air humidity and temperature as well as cloud formation. The low-frequency variability of drought was modulated by climate indices (Özger et al. 2009) from which El Niño-Southern Oscillation (ENSO) is known to dominate the signal of drought development across the globe (Vicente-Serrano et al. 2011; Guguloth et al. 2024). During warm ENSO phases, the region experienced the most severe dry events given the delay in the establishment of the rainy season and the significant precipitation deficit associated with these events. During the occurrence of dry events, agricultural production decreases, which generates severe economic damage to the region with the associated reduction in agricultural goods exports and leads to unemployment (Jodhani et al. 2021).

Global warming is a major phenomenon of climate change that has a significant impact on global and regional rainfall patterns (Omar et al. 2017; Gupta, N. et al. 2021). The 5th Assessment Report (AR5) (2014) of the Intergovernmental Panel on Climate Change (IPCC), based on scientific assessment (Alexander 2016) indicated a significant increase of mean global (ocean and land) average temperature by 0.85°C during 1800–2012, and it would further increase between 1.4°C to 5.8°C by the last quarter of the 21st century. When discussing the causes of drought, it's important to consider a range of environmental and human factors. It is caused by a combination of environmental and human factors. Climate change, with its rising temperatures and altered precipitation patterns, plays a significant role, alongside natural variability such as El Niño and La Niña (Gupta S.K. et al. 2021; Gupta et al. 2024). Environmental factors like soil moisture depletion and deforestation further exacerbate the issue. Human activities, including overuse and inefficient management of water resources, poor agricultural practices, urbanization, and pollution, also contribute to drought conditions. Additionally, feedback mechanisms like desertification and heatwaves can worsen the situation, creating a complex interplay between natural and anthropogenic influences.

General Circulation Model (GCM) runs are generally used for a better scientific understanding of the large-scale climate variation (Dixon et al. 2016; Gupta et al. 2023) and global warming effects for future periods. GCMs provide information that confirms that increasing the concentration of GHGs will have significant effects on global and regional scales. Recent studies show that internal climate variability dominates the signal of drought in north-central India. The rainfall deficit of the 2015–2019 event was likely exacerbated by anthropogenic climate change, highlighting the need to improve the capacity for climate change attribution studies (Jodhani et al. 2023). The identification of drought at such a local scale

is complex and typically hindered by quality data availability. This work explores the behavior of the drought events in the Uttar Pradesh region based on historical records and evaluates the potential for drought development under warming conditions, providing information that can be useful to support water resources management and policymaking (Jodhani et al. 2024). The analysis explores the observed influence of deficit in precipitation for drought development based on historical long-term records to determine the occurrence of meteorological and agricultural drought in the region and evaluates the impact of PET estimation in evaluating agricultural drought distribution. Based on the historical observations, the impact of ENSO on drought development, intensity, and spatial distribution was studied. Based on statistical downscaled products available from (Gupta et al. 2022), projected drought behavior was analyzed for future climate scenarios under Representative Concentration Pathways (RCP) 4.5 and 8.5.

2. STUDY AREA

Uttar Pradesh (U.P.) is India's fourth largest state, both in terms of area and population. Encompassing 243,286 km², which accounts for 7.33% of India's total land area, it is situated in the north-central region of the Gangetic plains. Its coordinates range from 23°52'N to 31°28'N latitudes and 77°30'E to 84°39'E longitudes. Bordered by nine other Indian states, U.P. shares its boundaries with Rajasthan to the west and east, Madhya Pradesh and Chhattisgarh to the south, Jharkhand to the southeast, and Bihar to the east. Additionally, it shares an international border with Nepal. Comprising 18 divisions, this study specifically focuses on synoptic stations including Agra, Aligarh, Azamgarh, Basti, Bareilly, Chitrakoot, Faizabad, Gorakhpur, Gonda, Jhansi, Kanpur, Meerut, Lucknow, Mirzapur, Moradabad, Prayagraj, Saharanpur, and Varanasi, as depicted in Figure 1. The state's geographical diversity leads to distinct climatic variations, as it extends from the Siwalik range in the southern foothills of the Himalayas to the Tarai belt in the north and is bordered by the Vindhyan Range and Plateau in the southern region (Bundelkhand and Bughelkhand). The central expanse of the state is occupied by the Indo-Gangetic plain. Mainly characterized by a humid subtropical climate (CWa), Uttar Pradesh experiences dry winters and exhibits regional diversity, particularly in its western part, where semi-arid (B.S.) conditions lead to higher evaporation than precipitation, resulting in cyclic drought scenarios. The state observes three distinct seasons, including Summer (March to May), which is marked by low humidity, hot and dry days, and occasional dust-laden winds, with temperatures sometimes soaring to 45°C or even 47 to 48°C. The Monsoon season (June to September) experiences an average annual precipitation of 990 mm, varying spatially from 501 to 1444.25 mm. Around 89% of the annual rainfall is attributed to the southwest monsoon, with July recording the highest rainfall, followed by August. The Tarai region receives substantial annual rainfall, with Gorakhpur and Behraich having the highest mean annual rainfall (1089–1245 mm), whereas the western part of the state, encompassing areas like Mathura, Auraiya, Rae Bareilly, Mahoba, and Bareilly, records comparatively lower average annual precipitation (464–620 mm). During the Winter season (October to January), temperatures drop to around 3–4°C, occasionally reaching as low as -1°C. Some parts of the state experience mild showers during the monsoon retreat.

Uttar Pradesh is home to a significant portion of India's population, with a staggering 199,812,341 residents. The state's economy is predominantly driven by agriculture, benefiting from its fertile landmass, which is crisscrossed by major rivers such as the Ganges, Yamuna, Gomati, and Gandak. Known as the rice bowl of India, this sector employs 7.7% of the state's workforce and plays a substantial role in both the state and national economies.

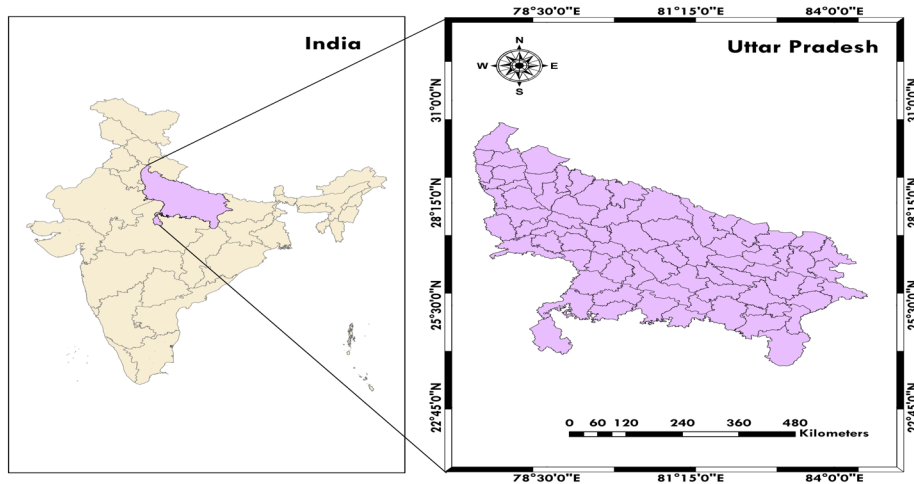


Figure 1 Map of India and Uttar Pradesh State map as a study area.

3. DATA AND METHODS

3.1 Data

Precipitation and temperature

The assessment of drought relies on two core meteorological factors: precipitation and temperature, which serve as input variables. To analyze the spatiotemporal nature of drought during the observed timeframe from 1971–2018, monthly records of precipitation and temperature were gathered. Daily data spanning from 1971–2005 were acquired from the Indian Meteorological Department (IMD). Furthermore, to evaluate drought characteristics from 2019 to 2050, simulated data was generated using the SDSM downscaling technique applied to the CanESM2 model. This process was conducted under three different RCP scenarios. The study also incorporated the use of the second-generation Canadian Earth System Model (CanESM2, covering the period 1961–2100) and 26 standardized large-scale surface and atmospheric predictor variables. These predictor variables were derived from the National Centers for Environmental Prediction (NCEP) reanalysis data spanning 1961–2005, all with a specific resolution scale, for the purposes of this research.

ENSO indices

Two ENSO indices were retrieved from the NOAA Earth Science Research Laboratory’s Physical Science Division (ESRL PSD) database, namely the Multivariate ENSO Index (MEI) and Niño 3.4. The MEI combines information on sea level pressure, sea surface temperature (SST), wind and outgoing long-wave radiation, and the Niño 3.4 index corresponds to the sea surface temperature (SST) anomaly in the region enclosed by 5N–5S and 120–170W.

3.2 Methods

Downscaling of CanESM2 model data using the SDSM under RCP scenarios

SDSM serves as a tool for downscaling rainfall from global climate models to regional levels. It utilizes both stochastic techniques and multiple linear regression (MLR). The initial step in SDSM involves

establishing a quantitative relationship between predicted and predictor variables. SDSM was further subdivided into three sub-models: yearly, seasonal, and monthly. Each of these models contributes to a regression equation. The annual sub-model generates a single equation for the entire year, while the seasonal sub-model develops equations separately for each season. Conversely, the monthly sub-model creates equations for each month separately. Additionally, the choice between conditional and unconditional sub-models depends on the type of parameter to be downscaled. Under the current conditions, the conditional model was appropriate for downscaling rainfall, while the unconditional model was suitable for downscaling temperature.

The screening of predictors represents a crucial stage in SDSM, wherein the selection of essential atmospheric parameters is determined through the MLR model. This model assesses P-values, histograms, scatter plots, correlation matrices, and partial correlations to identify the most appropriate predictors. In this study, a correlation matrix was employed to establish connections between predictors and CanESM2 predictors. Among highly correlated predictors, those demonstrating the best scatter plot and lowest P-value were meticulously chosen for rainfall prediction. All stations were equipped to measure precipitation (PRCP), surface-specific humidity (SHUM), and wind speed at 500 hPa. PRCP emerged as the most pivotal predictor across all stations, indicating its suitability for the area. Model calibration utilized data spanning 25 years from 1971–1995, with the subsequent period from 1996–2005 serving for model verification. For daily rainfall downscaling, the SDSM method was employed to develop the model. Utilizing the conditional sub-model, a regression equation was applied monthly to all 18 stations. Among optimization methods in SDSM, Ordinary Least Square (OLS) and Dual Simplex Optimization (DSO) were considered, with OLS being preferred due to its faster execution. During calibration and validation, root mean square error (RMSE) and coefficients of correlation (R^2) were employed to assess the performance of historical and simulated data. Based on NCEP and CanESM2 predictions, the model simulates daily rainfall for the period 1996–2005 using the model's calibration data from 1976–1995. From 1996–2005, various ensembles were used to derive the average, which was then validated with observed data. The model overestimated rainfall at every station during calibration. With the help of a biased correction, this overestimation is resolved.

Estimation of ET_0

Monthly temperature was used to compute reference evapotranspiration (ET_0) based on the Hargreaves approximation (Hargreaves 1994) given that wind and radiation information are not available for most of the stations.

$$ET_0 = 0.0023 * RA * (T_{\circ C} + 17.8) * T_D^{0.50} \quad (1)$$

Where:

RA = extraterrestrial radiation,

$T_{\circ C}$ = average of maximum and minimum temperatures, and

T_D = difference between maximum and minimum mean temperature.

The Hargreaves estimation was proposed as an alternative to the measurement of ET_0 using extraterrestrial radiation (RA), the difference between maximum and minimum mean temperature (T_D), and the average of maximum and minimum temperatures ($T_{\circ C}$). The estimates are based on monthly scales and radiation is computed as a function of latitude (Maidment 1993). The SPEI R library was used to compute ET_0 . For those stations for which more variables were available, ET_0 was estimated using the

Penman-Monteith approximation, and performing a correction of the radiation information using the approximation based on Julian day.

$$E_a = \frac{R_n \Delta + \frac{\rho C_p \delta_e}{r_a}}{\lambda [\Delta + \gamma (1 + r_s / r_a)]} \quad (2)$$

Where:

- R_n = net radiation ($W m^{-2}$),
- ρ = air density ($kg m^{-3}$),
- C_p = air-specific heat at constant pressure ($J kg^{-1} °C^{-1}$),
- δ_e = vapor pressure deficit (mbar),
- Δ = saturated vapor pressure gradient ($mbar °C^{-1}$),
- γ = psychrometric constant ($mbar °C^{-1}$),
- λ = vaporization latent heat ($J kg^{-1}$),
- r_a = aerodynamic resistance ($s m^{-1}$), which is a function of $208/U_2$, where U_2 is the wind speed at two meters height, and
- r_s = surface resistance ($s m^{-1}$) and depends on the leaf area.

For r_a , due to the lack of data availability, the reference value of $50 s m^{-1}$ was used, while for r_s the used value was $69 s m^{-1}$. The meteorological stations are in farmland areas, mostly dedicated to cattle grazing, so the soils are dominantly covered by grass and the simplification of $K_c \sim 1$ is considered so that $E_a \cong ET_0$, the estimation based on the above-mentioned constants is considered as valid.

Drought indices

Daily historical records were used to determine monthly values, which were then used to compute the Standardized Precipitation Evapotranspiration Index (SPEI). SPEI is an indirect method developed to evaluate drought, and it relates the monthly climate balance, the difference between precipitation and evapotranspiration water, as a measurement of the deficit or surplus of water. The evaluation of SPEI allows the use of different timescales, enabling the analysis of the length and propagation of drought across the hydrological system (Vicente-Serrano et al. 2011). The SPEI R library was used for the estimation of the index, previously considering the monthly climate balance as input for the estimation, the index was estimated for 1, 2, 3, 6, 9, and 12 months. The Standardized Precipitation Index (SPI) (McKee et al. 1993) was also estimated. It determines dry periods based on rainfall deficits. The historical precipitation records were adjusted to a normal probability distribution in which zero corresponds to the normal value, and negative (positive) values indicate dry (wet) periods. The estimates of different time scales reflect the impact of the drought on the surface water availability in short time scales and in longer time scales. SPI values are grouped into 7 categories, and the SPEI R library was used for their estimation. SPI and SPEI are favored for drought estimation over other indices due to their standardized approach and versatility. SPI relies solely on precipitation data, making it simple and adaptable across regions and time scales. SPEI includes both precipitation and temperature, offering a comprehensive assessment, especially under climate change. This combination provides robust and complementary insights into drought conditions.

4. RESULTS AND DISCUSSION

4.1 Drought events and ENSO impact based on historical observations

Evapotranspiration (ET)

Analysis of extreme precipitation is known to be hindered by the availability of observational records. Although the identification of meteorological drought can be conducted based on available precipitation data, the assessment of agricultural drought is the capacity to estimate ET as the main component of the water balance and key in the surface-atmosphere coupling which defines the transport of water fluxes. Reference evapotranspiration (ET_0) was estimated using the Hargreaves and Penman-Monteith methods; estimates based on the Hargreaves method present as approximately uniform throughout the year because of the weight extra-terrestrial radiation data has in the estimation. Because long-term records are often limited to precipitation and temperature information, estimations that include wind and radiation do not often exist. In a water-limited environment, as is the case for semi-arid regions, an increase in rainfall is associated with larger latent heat fluxes due to the increase in moisture and a decrease in the shortwave radiation due to increasing cloudiness and moisture. During the dry season, ET_0 is lower due to the influence of reduced water availability and lower surface temperature as less cloudiness enables larger portions of long-wave radiation to escape back to space. As the transition from the dry to the wet season is established, ET_0 peaks. Based on the estimations for the Uttar Pradesh region stations, differences of 100 mm/month were identified between the Hargreaves and Penman-Monteith estimates during the rainy season. Such differences may be associated with the limitation of Hargreaves estimation as it neglects the cloudiness conditions typical of the rainy season, and consequently the humidity profiles. Hargreaves-based estimation shows an overestimation of ET_0 compared to Penman-Monteith estimates and shows a smoothed annual cycle. Penman-Monteith estimates of ET_0 show that maximum ET_0 values between November and April coincide with the drier months over the Pacific slope with a peak in March (~113 mm/month). From May to November, atmospheric evaporation potential is reduced, in part due to the increase in cloudiness which limits the amount of incoming solar radiation. As a result, the energy required to increase the amount of water vapor decreases, and ET_0 slightly increases during the MSD, and minimum values are observed during June (~44 mm/month) and September (~31mm). In the context of drought dynamics, ET_0 importance lies in the energy feedback represented by latent heat fluxes and the transfer of water in the form of vapor which contributes to warming the surface. High temperatures are associated with increases in ET_0 , the consequent loss of soil moisture, and a likely decrease in precipitation. Hence, understanding the behavior of ET with respect to ET_0 and its response to climate variability and warming scenarios is fundamental to better assess drought occurrence and impacts in the Uttar Pradesh region of India.

Drought characteristics under observed period

SPEI time series estimated for the future period (2019–2050), respectively, using CanESM2 data downscaled using SDSM across 18 synoptic stations of Uttar Pradesh under RCP 4.5 and RCP 8.5. All the study locations will experience an increase in temperature with varies spatially. This will eventually lead to an increase in PET across the entire study area. Another result drawn from precipitation downscaling was that precipitation will gradually increase in the near future, with significant variations: 66% of the locations will see an increase in precipitation of less than 10% over the study area. The study region will be vulnerable to the concurrent occurrence of dry and wet events in the near future as a slow increase in precipitation combines with a significant rise in temperatures. This present study assessed drought

characteristics by employing a run theory at SPEI <-1 threshold based on the severity, duration, and frequency. The research area's southwestern, Bundelkhand, and Vindhyan regions are more severely hit by severe drought conditions. Drought conditions in the Bundelkhand and Vindhyan regions are getting worse because of the local geology. Bundelkhand and Vindhyan regions are largely covered with hills and plains, and they are characterized by severe temperatures and a lack of rainfall. These regions of the study area are characterized by a semi-arid climate and a meteorological drought with a 3-year return time (Figure 2). As a result, meteorological drought has a major impact on this region, in particular. Therefore, in this section, the Agra, Jhansi, and Mirzapur locations were chosen to depict the change in drought characteristics across the observed and projected periods. Decadal variability of meteorological drought episodes was assessed using SPEI and SPI at various accumulation periods of the climate variable on time scales of 3-months, 6-months, 9-months, and 12-months for five decades: 1970s, 1980s, 1990s, 2000, and 2010s in Uttar Pradesh. At the SPI/SPEI-1 threshold, the number of drought events was calculated for several categories ("Moderate," "Severe," and "Extreme").

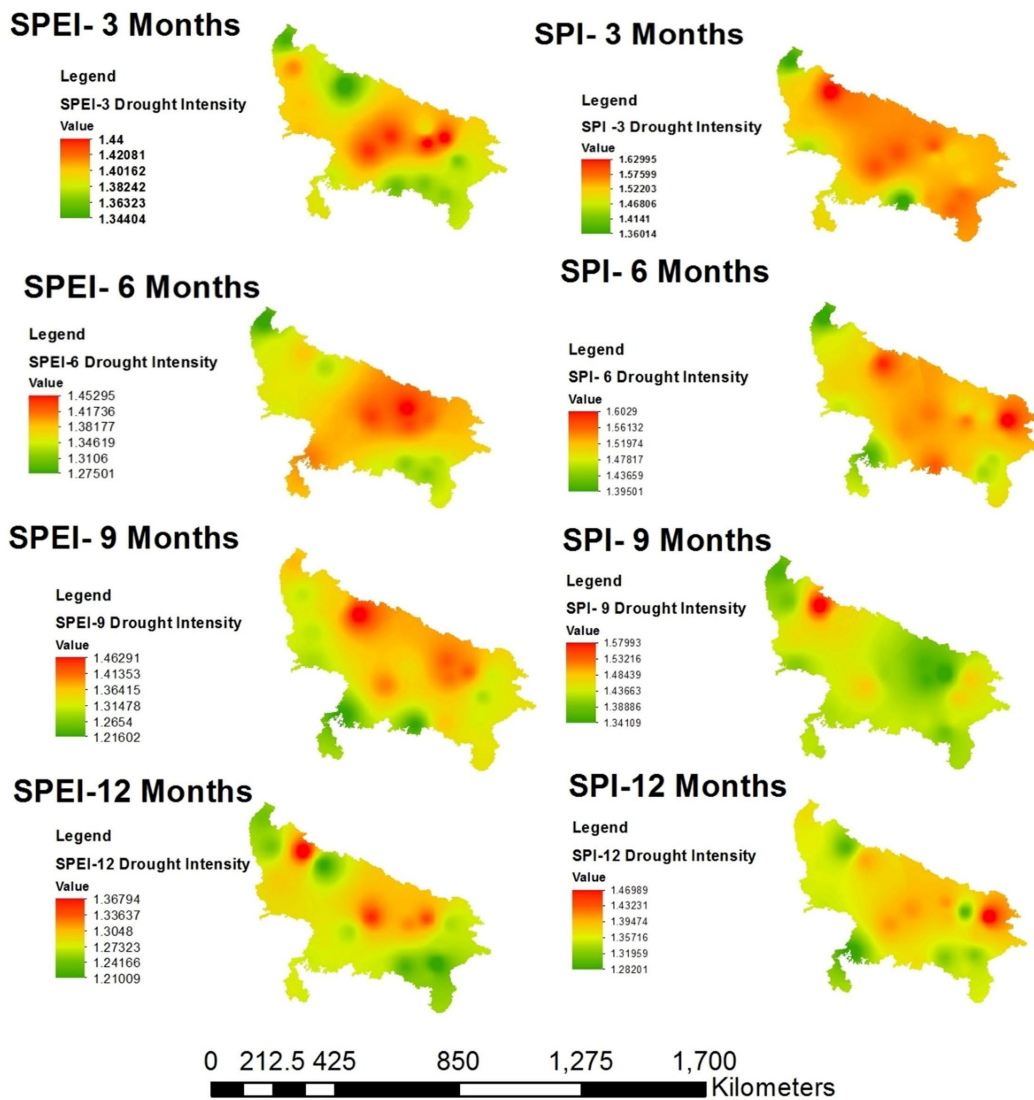


Figure 2 Spatial distribution of the drought intensity for a scale of 3-months, 6-months, 9-months, and 12-months.

4.3 Drought under warming scenario

The SPEI time series for precipitation and temperature have been estimated using CanSEM2 data that has been downscaled using SDSM to evaluate the impact of warming and changing climate on drought characteristics under the different climate projections of RCP 4.5 and RCP 8.5 for the next 32 years between 2019 and 2050. Drought frequency is based on SPEI with a run theory estimated at an SPEI <-1 threshold according to the different scenarios of RCP 4.5, and RCP 8.5, respectively. Figure 3 depicts the spatial variability of drought frequency estimated at different timescales for the 18 synoptic locations in Uttar Pradesh from 2019–2050 under RCP 4.5, and RCP 8.5. There was a change in the spatial pattern and magnitude of frequency occurrence recognized at different scales of SPEI. SPEI time series projected under RCP 4.5 and RCP 8.5 scenarios demonstrate that droughts occur with a higher frequency at shorter time scales (SPEI-3 and SPEI-6), whereas at a longer time scale, they show a significant drop in the frequency of drought events with SPEI-9 and SPEI-12. All 18 locations will experience an amplification of drying events in the future, and under this changing climate circumstance drought characteristics also exhibit a significant variance spatially under RCP 4.5 and RCP 8.5 scenarios. Under RCP 4.5 scenarios, the drought frequency was higher, at over 77% of synoptic locations compared to the RCP 8.5 scenarios. The magnitude and spatial extension of drought events decrease with an increasing SPEI timescale. The spatial distribution map of drought frequency demonstrates that the study region was likely to experience more frequent drought occurrences from 2019 to 2050 under the RCP 4.5 scenario than under RCP 8.5. Drought frequency at shorter time scales (SPEI-3 and SPEI-6) under RCP 4.5 and RCP 8.5 scenarios show that the frequency of occurrence varies spatially (Figures 3(a) and (b)). Compared to other areas in the study area, the eastern plain stretching along the Vindhyan region and the Bundelkhand region of Uttar Pradesh was likely to experience more frequent drought occurrences under RCP 4.5. However, under RCP 8.5, these regions will likely see more frequent episodes of droughts with smaller magnitudes than under RCP 4.5. Drought frequency under RCP 4.5 and RCP 8.5 scenarios for longer time scales (SPEI-9 and SPEI-12) are portrayed in Figures 3(c) and (d), exhibiting the different regional patterns of drought frequency. The drought frequency declined significantly under the RCP 4.5 scenarios of SPEI-9 and SPEI-12 time series to 2.4 and 1.5, respectively. Varanasi, Meerut, Mirzapur, Jhansi, Lucknow, Azamgarh, and Bareilly have a higher incidence of drought in the SPEI-9 time series compared to the other synoptic stations. As the spatial map depicts, drought frequency was expected to increase over the synoptic locations of Agra, Varanasi, Azamgarh, Bareilly, and Kanpur for the SPEI-12 time series. Under the RCP8.5 scenario, for SPEI-9 time series, compared to the rest of the synoptic stations, drought frequency was greater at Varanasi, Azamgarh, Meerut, Saharanpur, Agra, Jhansi, and Mirzapur. For the SPEI-12 time series, drought frequency increases over the synoptic locations of Varanasi, Saharanpur, Azamgarh, and Jhansi. The red color on the spatial map region represents the region with higher frequency. The spatial map of SPEI-12 shown in Figure 3(d) clearly demonstrates that the region with greater frequency was not likely to affect a large portion of the study region. Long-term drought will be less prevalent in the research area in the future. The spatial map demonstrates that most of the study area will be less likely to experience drought on a longer time scale, specifically at the SPEI-12 time series. The study region was majorly impacted by the frequent occurrence of short-term droughts. The frequency of drought events in the study area increases under RCP 4.5 scenarios compared to RCP 8.5 at nearly all scales.

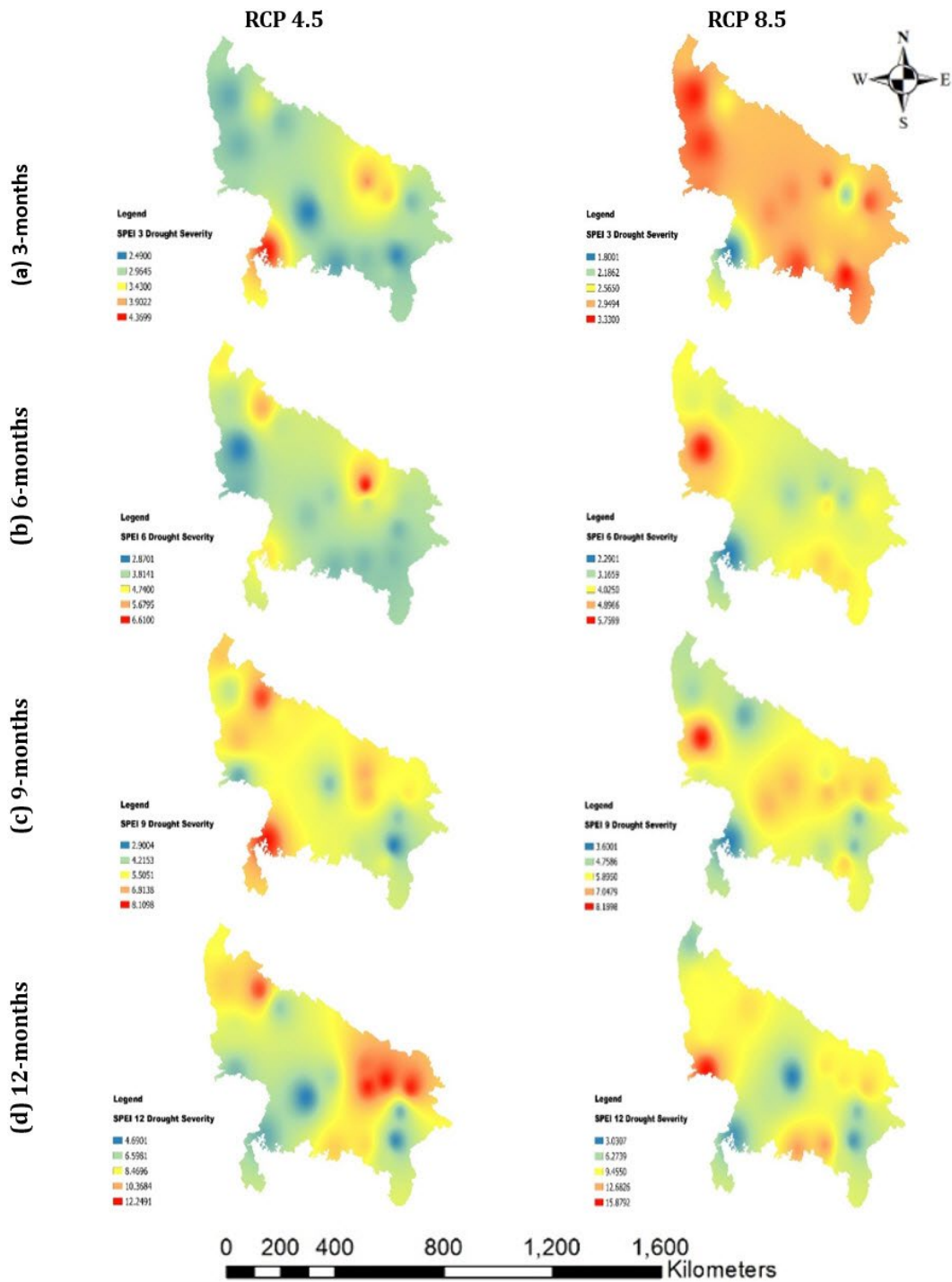


Figure 3 Spatial distribution of the drought severity over the study area at different timescales of SPEI time-series: (a) 3-months, (b) 6-months, (c) 9-months, and (d) 12-months, under RCP 4.5 and RCP 8.5 for the future period (2019 to 2050).

4.4 Impact of ENSO over observed drought events

An ENSO warm phase was associated with the warming of the equatorial Pacific waters and changes in the atmospheric pressure which result in variations of global circulation patterns. The link between ENSO

and drought corresponds to the hydrological response and soil moisture conditions (Vicente-Serrano et al. 2011). To accurately determine the impact ENSO has on the different types of droughts is difficult given the delayed response of vegetation and the groundwater systems to the reduction of precipitation and to the scarcity of vegetation and soil moisture depth at the local scale. Warm ENSO was associated with a reduction in precipitation on the Pacific slope, and the Uttar Pradesh region was known for drought development linked to the ENSO warm phase. Warm ENSO results in quasi periodic meteorological drought events, with the second leg of the rainy season (ASON) corresponding to the months more affected by the persistence of negative precipitation anomalies.

The trend and shift patterns of the selected variables were assessed during the monsoon across four different combinations of the ENSO phases: (1) El Niño years, (2) La Niña years, (3) non-El Niño years (including La Niña or neutral years), and (4) non-La Niña years (including El Niño or neutral years). The ENSO (Niño 3.4) indices utilized in this study (Figure 4) were obtained from the online database of the United States National Oceanic and Atmospheric Administration. Throughout the 102-year study period, 37 instances were identified as neutral years, 32 instances as El Niño years, and 33 instances as La Niña years. Consequently, a total of 70 instances constituted non-El Niño years, while 69 instances constituted non-La Niña years.

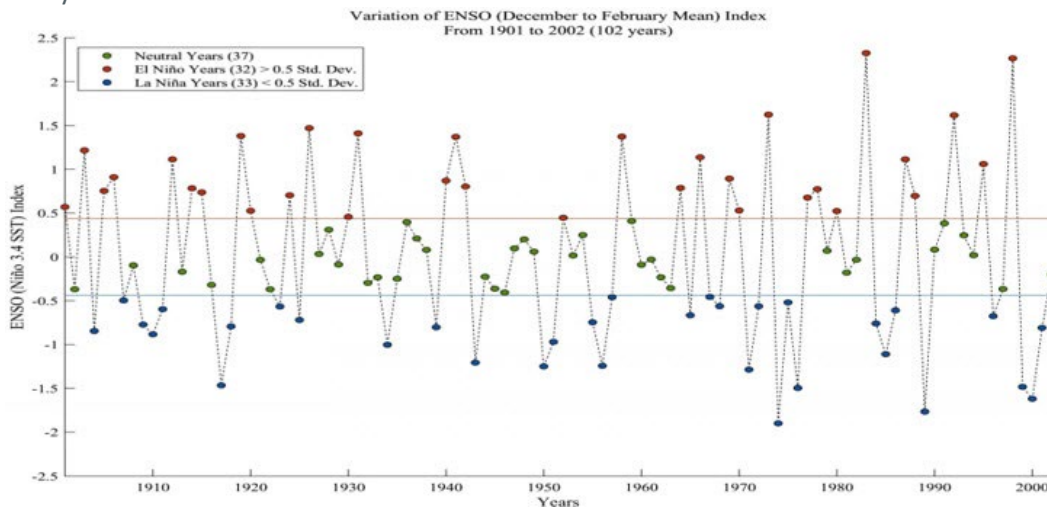


Figure 4 ENSO (Niño 3.4) index variations over the study period, with orange and blue horizontal lines indicating thresholds for El Niño and La Niña conditions, respectively.

In this sense, extensive mono-crops are common in the areas that were found to be more affected by the propagation of the drought. Despite the fact that this study did not consider the impact irrigation may have, albeit it was mentioned that irrigation may play a role in the lack of response of NDVI to the drought propagation, the fact that most agricultural drought events were identified in areas with extensive farming may imply more irrigation was required to maintain the crops, causing further impacts on the availability of water for the communities and contributing to the overexploitation of groundwater resources. Hence, mitigation measures can be proposed for the agricultural lands in the middle Ganges River basin such as improving permanent vegetation coverage to buffer the propagation of the meteorological to agricultural drought.

5. LIMITATIONS

Uncertainties in future projections and observational data arise from various sources. Observational datasets can suffer from measurement errors, data quality inconsistencies, limited spatial and temporal coverage, and issues with historical data homogeneity. Climate models introduce uncertainties through differences in model structure, parametrization, initial conditions, internal variability, emission scenarios, and feedback mechanisms. Additionally, regional downscaling adds another layer of complexity. Drought indicators like SPI and SPEI have limitations; SPI relies solely on precipitation data, potentially missing critical temperature and evapotranspiration effects, while SPEI's incorporation of temperature makes it more complex and sensitive to varying climatic conditions. These factors must be considered to accurately interpret drought assessments and projections.

6. CONCLUSION

This study assesses historical drought in Uttar Pradesh and evaluates future drought behavior using regional statistically downscaled climate projections. It highlights the importance of identifying drought types to better inform water resource management. Key findings include the scarcity of high-quality long-term records, limiting drought analysis to interannual variability, and the inability to detect trends in drought frequency and intensity due to record length and regional spatial variability. However, consistent warming trends suggest increased atmospheric demand, impacting drought intensity. The study notes a higher atmospheric demand in southern Uttar Pradesh, contributing to water deficits. Albeit the impact of El Niño was more significant during the second leg of the rainy season, because the teleconnection pattern affects the development of synoptic systems and their interaction with the Inter-Tropical Convergence Zone, reducing the amount of rainfall in the region, the impact prolongates during the dry season and increases the propagation of the drought across the hydrological cycle compartments. As a result, prolonged drought exacerbates the problem of water resources availability and the pollution of aquifers. Statistical downscaled climate projections show consistency in increasing temperatures, with the Bundelkhand experiencing the largest temperature increase, and a generalized rainfall decrease was projected for the same, with the Chambal River basin and the Uttar Pradesh projected to experience the most significant precipitation reduction. Future climate scenarios draw attention to the potential decrease in rainfall and probable intensification of dry conditions towards the end of the century, posing a major threat for the rain-fed agricultural activities developed in the irrigation district area. Challenges include data scarcity, model limitations in representing small-scale surface processes, and the need for better integration of data and models to understand drought dynamics. Improving spatial resolution and monitoring systems is crucial for accurate climate scenario projections and informed decision-making.

ACKNOWLEDGMENTS

The author Nitesh Gupta acknowledges the support of Nirma University. The author Padam Jee Omar expresses sincere thanks to the Department of Civil Engineering, Babasaheb Bhimrao Ambedkar University (A Central University), Lucknow, India.

REFERENCES

- Alexander, L.V. 2016. "Global observed long-term changes in temperature and precipitation extremes: a review of progress and limitations in IPCC assessments and beyond." *Weather and Climate Extremes* 11, 4–16.
- Chaware, S., S.M. Taley, and S.U. Jadhav. 2017. "Performance of different methods of estimating potential evapotranspiration in western Vidarbha region." *Contemporary Research in India* 7 (3): 417–420.
- Cooley, S.S., C.A. Williams, J.B. Fisher, G.H. Halverson, J. Perret, and C.M. Lee. 2018. "Assessing regional drought impacts on vegetation and evapotranspiration: A case study in Guanacaste, Costa Rica." *Ecological Applications* 29 (2): 1–21.
- Dixon, K.W., J.R. Lanzante, M.J. Nath, K. Hayhoe, A. Stoner, A. Radhakrishnan, V. Balaji, and C.F. Gaitán. 2016. "Evaluating the stationarity assumption in statistically downscaled climate projections: is past performance an indicator of future results?" *Climate Change* 135, 395–408.
- Gaur, S., P.J. Omar, and S. Eslamian. 2023. "Advantage of grid-free analytic element method for identification of locations and pumping rates of wells." In: S. Eslamian, F. Eslamian (Eds.), *Handbook of Hydroinformatics: Vol: III*, p. 1–10. Elsevier.
<https://doi.org/10.1016/B978-0-12-821962-1.00003-9>
- Goldin, T. 2016. "India's drought below ground." *Nature Geoscience* 9, 98–98
- Gond, S., N. Gupta, J. Patel, and P.K.S. Dikshit. 2023. "Spatiotemporal evaluation of drought characteristics based on standard drought indices at various timescales over Uttar Pradesh, India." *Environmental Monitoring and Assessment* 195, 439.
- Guguloth, S., and M. Pandey. 2023. "Accuracy evaluation of scour depth equations under the submerged vertical jet". *AQUA-Water Infrastructure, Ecosystems and Society* 72 (4): 557–575.
- Guguloth, S., M. Pandey, and M. Pal. 2024. "Application of Hybrid AI Models for Accurate Prediction of Scour Depths under Submerged Circular Vertical Jet." *Journal of Hydrologic Engineering* 29 (3): 04024010.
- Gupta, L.K., M.R. Bharadwaj, and M. Pandey. 2024. "Comparative study of reduction of pier scour using octagonal and circular collars." *Ocean Engineering* 298, 117169.
- Gupta, N., A. Banerjee, and S.K. Gupta. 2021. "Spatio-temporal trend analysis of climatic variables over Jharkhand, India." *Earth Systems and Environment* 5 (1): 71–86.
- Gupta, N., P.K. Mahato, J. Patel, P.J. Omar, and R.P. Tripathi. 2022. "Understanding trend and its variability of rainfall and temperature over Patna (Bihar)". In: M. Zakwan, A. Wahid, M. Niazkar, U. Chatterjee (Eds.), *Current Directions in Water Scarcity Research* (Vol. 7, pp. 533–543). Elsevier.
<https://doi.org/10.1016/B978-0-323-91910-4.00030-3>
- Gupta, N., J. Patel, S. Gond, R.P. Tripathi, P.J. Omar, and P.K.S. Dikshit. 2023. "Projecting Future Maximum Temperature Changes in River Ganges Basin Using Observations and Statistical Downscaling Model (SDSM)." In: Pandey, M., Azamathulla, H., Pu, J.H. (eds), *River Dynamics and Flood Hazards. Disaster Resilience and Green Growth*. Springer, Singapore. https://doi.org/10.1007/978-981-19-7100-6_31

- Gupta, S.K., N. Gupta, N. and V.P. Singh. 2021. "Variable-Sized Cluster Analysis for 3D Pattern Characterization of Trends in Precipitation and Change-Point Detection." *Journal of Hydrologic Engineering* 26 (1): 04020056.
- Jain, R., K. Timani, and M. Pandey. 2023. "Influence of cohesion on California bearing ratio of clay–gravel mixtures." *International Journal of Sediment Research* 38 (3): 374–386.
- Jain, V.K., R.P. Pandey, and M.K. Jain. 2015. "Spatio-temporal assessment of vulnerability to drought." *Natural Hazards* 76, 443–469.
- Jee, O.P., D.S. Bihari, and D.P. Kumar. 2019. "Temporal variability study in rainfall and temperature over Varanasi and adjoining areas." *Disaster Advances* 12 (1): 1–7.
- Jodhani, K., P. Bansal, and P. Jain. 2021. "Shoreline Change and Rate Analysis of Gulf of Khambhat Using Satellite Images." *Advances in Water Resources and Transportation Engineering*, Conference Paper, 151–70. https://doi.org/10.1007/978-981-16-1303-6_12
- Jodhani, K.H., D. Patel, N. Madhavan, and S.K. Singh. 2023. "Soil Erosion Assessment by RUSLE, Google Earth Engine, and Geospatial Techniques over Rel River Watershed, Gujarat, India." *Water Conservation Science and Engineering* 8 (1): 49. <https://doi.org/10.1007/s41101-023-00223-x>
- Jodhani, K.H., H. Patel, U. Soni, R. Patel, B. Valodara, N. Gupta, et al. 2024. "Assessment of Forest Fire Severity and Land Surface Temperature using Google Earth Engine: A Case Study of Gujarat State, India." *Fire Ecology* 20 (1): 23. <https://doi.org/10.1186/s42408-024-00254-2>
- McCabe, M.F., D.G. Miralles, T.R. Holmes, and J.B. Fisher. 2019. "Advances in the Remote Sensing of Terrestrial Evaporation." *Remote Sensing* 1138.
- McKee, T.B., N.J. Doesken, and J. Kleist. 1993 "The relationship of drought frequency and duration to time scale." In: *Proceedings of the Eighth Conference on Applied Climatology*, Anaheim, California, 17–22 January 1993. Boston, American Meteorological Society, 179–184.
- Meza, I., S. Siebert, P. Döll, J. Kusche, C. Herbert, E.E. Rezaei, et al. 2020. "Global-scale drought risk assessment for agricultural systems." *Natural Hazards and Earth System Sciences* 20 (2): 695–712.
- Miralles, D., P. Gentile, S.I. Seneviratne, and A.J. Teuling. 2019. "Land-atmospheric feedbacks during droughts and heatwaves: State of the science and current challenges." *Annals of the New York Academy of Sciences* 1436 (1): 1–17.
- Mishra, A.K., and V.P. Singh. 2010. "A review of drought concepts." *Journal of Hydrology* 391, 202–216.
- Mishra, V., S. Aadhar, A. Asoka, S. Pai, and R. Kumar. 2016. "On the frequency of the 2015 monsoon season drought in the Indo-Gangetic Plain". *Geophysical Research Letters* 43, 12102–12112
- Mishra, V., A.D. Tiwari, S. Aadhar, R. Shah, M Xiao, D.S. Pai, et al. 2019. "Drought and Famine in India, 1870–2016." *Geophysical Research Letters* 46 (4): 2075–2083.
- Monteith, J.L. 1965. "Evaporation and environment, in the state and movement of water in living organisms." *Symp. Soc. Exp. Biol*, 205–234. Academic Press.
- Omar, P.J., N. Gupta, R.P. Tripathi, and S. Shekhar. 2017. "A study of change in agricultural and forest land in Gwalior city using satellite imagery." *SAMRIDDHI: A Journal of Physical Sciences, Engineering and Technology* 9 (02):109–112.

- Omar, P.J., and V. Kumar. 2021. "Land surface temperature retrieval from TIRS data and its relationship with land surface indices." *Arabian Journal of Geosciences* 14 (18): 1897. <https://doi.org/10.1007/s12517-021-08255-0>
- Özger, M., A.K. Mishra, and V.P. Singh. 2009. "Low frequency drought variability associated with climate indices." *Journal of Hydrology* 364 (1-2): 152–162.
- Pandey, M., M. Karbasi, M. Jamei, A. Malik, and J.H. Pu. 2023. "A Comprehensive Experimental and Computational Investigation on Estimation of Scour Depth at Bridge Abutment: Emerging Ensemble Intelligent Systems" *Water Resources Management*, 1–23.
- Pandey, P., A.R. Mishra, P.K. Verma, and R.P. Tripathi. 2022. "Study and implementation of smart water supply management model for water drain region in India". In: *VLSI, Microwave and Wireless Technologies: Select Proceedings of ICVMWT 2021*, 711-721. Springer Nature, Singapore.
- Schwalm, C.R., W.R. Anderegg, A.M. Michalak, J.B. Fisher, F. Biondi, G. Koch, et al. 2017. "Global patterns of drought recovery." *Nature* 548 (7666): 202–205.
- Singh, K., P. Pandey, S. Pandey, A. Mishra, and R. Tripathi. 2022. "AI-based water quality monitoring of the river Ganges using fuzzy". *LARHYSS Journal* P-ISSN 1112-3680/E-ISSN 2521-9782 (51): 67–85.
- Srivastava, S., P.J. Omar, S. Shekhar, and S. Gupta. 2023. "Study of acidic air pollutant (SO₂ and NO₂) tolerance of microalgae with sodium bicarbonate as growth stimulant." *AQUA-Water Infrastructure, Ecosystems and Society* 72 (5): 739–749. <https://doi.org/10.2166/aqua.2023.013>
- UNICEF. 2016. Drought in India 2015–2016: When coping crumbles—A rapid assessment of the impact of drought on children and women in India—India | ReliefWeb. <https://reliefweb.int/report/india/drought-india-2015-16-when-coping-crumbles-rapid-assessment-impact-drought-children-and>. Accessed 27 Feb 2022.
- Van Loon, A.F., G. Laaha. 2015. "Hydrological drought severity explained by climate and catchment characteristics." *Journal of Hydrology* 526, 3–14.
- Van Loon, A.F., K. Stahl, G. Di Baldassarre, J. Clark, S. Rangelcroft, N. Wanders, et al. 2016. "Drought in a human-modified world: reframing drought definitions, understanding, and analysis approaches." *Hydrological Earth Systems Science* 20, 3631–3650.
- Vicente-Serrano, S.M., J.I. López-Moreno, L. Gimeno, R. Nieto, E. Morán-Tejeda, J. Lorenzo-Lacruz, et al. 2011. "A multi-scalar global evaluation of the impact of ENSO on droughts." *Journal of Geophysical Research: Atmospheres* 116 (D20).